ADVANCED FUNCTIONAL MATERIALS
www.afm-journal.de

www.MaterialsViews.com

Complexation-Induced Biomimetic Long Range Fibrous Orientation in a Rigid-Flexible Block Copolymer Thermogel

*Min Hee Park, Bo Gyu Choi, and Byeongmoon Jeong**

The orientation of the organofibrous structure plays an important role not only in the biomineralization process but also in the extracellular matrix (ECM) of articular cartilage by providing cells with biomechanical cues. Here, it is reported that a long range nanofibrous orientation can be realized by a self-assembling ionic complex between (+)-charged amphiphilic peptide block copolymers with a rigid-flexible block structure (polyalanine-PLX-polyalanine; PA-PLX-PA) and (-)-charged hyaluronic acid (HA). A biomimetic 3D culture system encapsulating chondrocytes is formed by a temperature-sensitive sol-to-gel transition of the PA-PLX-PA/HA complex aqueous solution, which provides a compatible microenvironment for the cells. The cell proliferation and biomarker expression for articular cartilage are significantly improved in the PA-PLX-PA/HA complex system relative to the PA-PLX-PA or the commercially available Matrigel systems. In particular, noticeable cell clustering is observed in the PA-PLX-PA/HA complex system with the long range nanofibrous structure. This research suggests a new method for developing a nanofibrous structure using an amphiphilic peptide block copolymer and demonstrates its potential uses as a unique biomimetic cell-culture matrix.

1. Introduction

Self-assembly of polymers to a specific nanostructure has been intensively investigated as a bottom-up design principle of biological or biomedical materials.[1–3] In this regard, biomimetic approach provides an elegant platform for materials scientists.[4] In particular, thermogels that undergo a solution (sol)-to-gel transition have been suggested to be a very promising due to their advantages such as simple sterilization, no surgical procedure being required for implantation, and irregular shaped defects being easily filled using the material.[5–8]

The extracellular matrix (ECM) is a 3D matrix of collagen fibres and proteoglycans, where the collagen fibres exist as nanofibrous bundles and proteoglycans are connected to hyaluronic acid (HA) through a link protein domain with 100 amino acids.[9] In articular cartilage, collagens and proteoglycans are oriented horizontally in the superficial zone, whereas they are oriented vertically in the deep zone. The orientation of the fibrous structure provides a surface with minimal friction in the superficial zone and stress-bearing capacity in the deep zone connected to bones.[10]

In this study, we developed a thermogelling complex system consisting of amphiphilic block copolymers with a rigid-flexible block structure and HA to mimic the biological structure of the HA-protein macroaggregates, where a long range nanofibrous orientation is expected to be produced by ionic interactions between the cationic ammonium end groups of β-sheeted peptide block polymers and anionic carboxylate groups along the HA (**Figure 1**). The hydrophobic blocks of the copolymer, polyalanine, not only supports the structural rigidity but also provides tight ionic interaction domains through its low dielectric constant (ε) by the Coulomb's law, $F = Q_1Q_2/(4\pi\varepsilon r^2)$, where Q_1 and Q_2 are the charges of the ions and F is the electrostatic force between the ions at a distance of r. ε of water is 78 and decreases in a hydrophobic domain.[11]

Thermogelling polymer systems including poly(lactic acid-*co*-glycolic acid)/poly(ethylene glycol) (PEG), olio(PEG fumarate), chitosan/glycerol phosphate, poly(*N*-isopropylacrylamide) derivatives, poly[*N*-(2-hydroxypropyl) methacrylamide lactate], etc. have been investigated for 3D culture of chondrocytes.[12–14] In all types of the 3D culture systems, chondrocytes preserved their spherical phenotypes and increased the expression of type II collagen relative to type I collagen. The biomarker expression increased by incorporating ascorbate, dexamethasone, and TGF-β3.[15] In particular, oligo(PEG fumarate) and PEG diacrylate were crosslinked in the presence of transforming growth factor (TGF)-β1 microspheres and chondrocytes.[16] 4–5 times increases in cell number and the production of the glycosaminoglycan were observed in the system over 28 days. A temperature-sensitive physical gelation, followed by additional chemical crosslinking of the methacrylate groups by photopolymerization, provided bioprintable mechanical properties to the gel, which allowed chondrocytes to be printed in the 3D gel matrix.[17] In polypeptide thermogels with different secondary structures, chondrocytes showed increased biomarker expression in a specific polypeptide gel, indicating that control of microenvironments is an important factor in the 3D culture of the chondrocytes.[18]

Our current system is unique in that biomimetic nanofibrous structures were introduced by ionic interactions between

M. H. Park, Dr. B. G. Choi, Prof. B. Jeong
Department of Chemistry and Nano Science
Department of Bioinspired Science (WCU)
Ewha Womans University
Seoul, 120-750, Korea
E-mail: bjeong@ewha.ac.kr

DOI: 10.1002/adfm.201201722

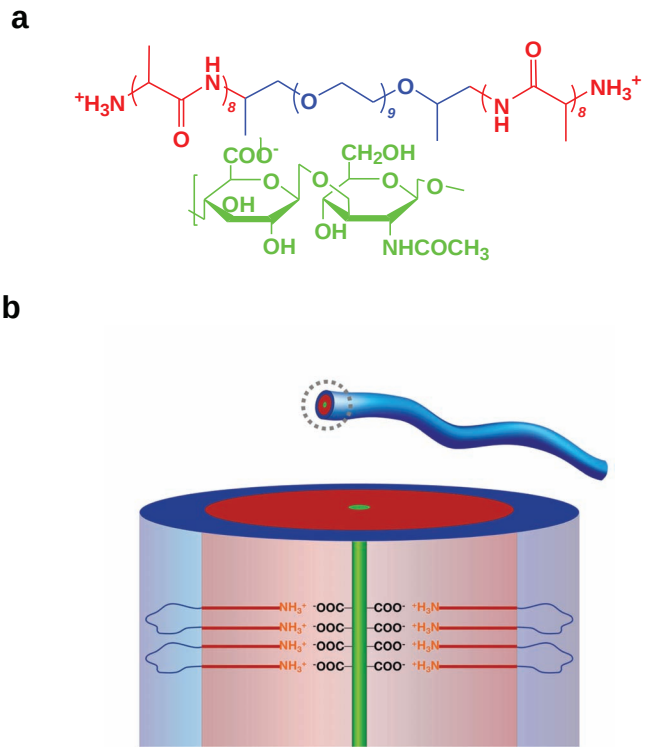

Figure 1. a) Chemical structure of PA-PLX-PA and HA. b) Complexation between the ammonium groups of PA-PLX-PA and carboxylate groups of HA. Thin blue lines, thick red lines, and thick green lines indicate the PLX, the PA, and the HA, respectively.

cationic rigid-flexible block polypeptides and anionic HA. Matrigel obtained by decellularization of rat tumor tissues is a commercially available thermogelling system, and was used as a control.

2. Results and Discussion

The amphiphilic block copolymer was synthesized by ring-opening polymerization[18,19] of N-carboxy anhydrides of L-alanine and *N*-carboxy anhydrides of DL-alanine on α,ω-diamino end capped poly(ethylene glycol) (PLX) with a structure of (propylene glycol)$_{1.8}$-(ethylene glycol)$_9$-(propylene glycol)$_{1.8}$. The polymer was purified by fractional precipitation to eliminate side products including homopolypeptides and unreacted PEG. First, the reaction products were dissolved in a good solvent (*N,N*-dimethyl formamide/chloroform cosolvent) and the undissolved fraction was filtered out, then the polymer was fractionally precipitated from the soluble fraction by slowly adding diethyl ether. Finally, the polymer was dialyzed using membrane (cut-off molecular weight 1000 Daltons) and freeze dried. Assuming the same reactivity of L and DL isomers during polymerization, the L/DL ratio of the alanine in the polymer was 60/40 (mole ratio). The unimodal molecular weight distribution of the polymer in the gel permeation chromatogram indicated that a well-defined polyalanine-PLX-polyalanine (PA-PLX-PA) was synthesized, and the ^{1}H-NMR spectra analyzed by the ratio of the area under the peaks at 1.2-1.8 ppm (CH_3 of PLX and Ala) and 3.6-4.1 ppm (CH_2 and CH of PLX) confirmed the composition and structure of the polymer to be (alanine)$_8$-PLX-(alanine)$_8$ (Figure S1, Supporting Information).

Both PA-PLX-PA and PA-PLX-PA/HA complex aqueous solutions underwent a sol-to-gel transition as the temperature increased. The moduli (G') of the aqueous solutions (8.0 wt%) were less than 1.0 Pascal (Pa) in the sol state at 4 °C, whereas G' of the thermogels at 37 °C prepared from the polymer aqueous solutions (8.0 wt%) varied over 1000–1600 Pa, 440–750 Pa, 270–400 Pa at HA contents of 0.0 wt%, 0.5 wt%, and 1.0 wt%, respectively (**Figure 2**a). The photographs of the sol (4 °C) and gel (37 °C) states of the PA-PLX-PA/HA complexes are shown in Figure 2b. The modulus of Matrigel in an aqueous solution was less than 0.1 Pa at 4 °C, and increased to 70–80 Pa in the gel phase at 37 °C. The low gel modulus of the Matrigel limits its application in 3D cell/stem cell cultures where a high level of rigidity is required.[18,20]

The cryo-transmission electron microscopy (cryo-TEM) image of the PA-PLX-PA gel at 37 °C in the absence of HA shows randomly oriented nanofibrous networks of the polymers (PHA0.0 in **Figure 3**a), whereas bundles of the nanofibrous structures with

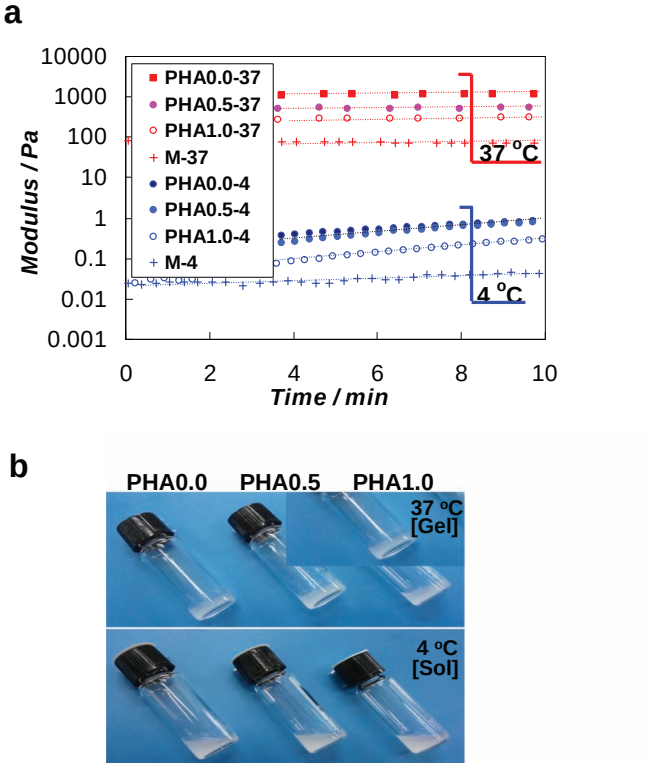

Figure 2. a) Modulus of the PA-PLX-PA aqueous polymer solutions (8.0 wt%) at 4 °C (blue) and their thermogels at 37 °C (red) as a function of HA content. PHA*x*-*y* in the legend indicates that *x* wt% of HA is incorporated in the PA-PLX-PA aqueous solution and the modulus of the polymer aqueous solution is measured at *y* °C. Matrigel (M) was compared as a control. The modulus increases more than 100 times by the sol (4 °C)-to-gel (37 °C) transition. b) The photographs of sol (4 °C) and gel (37 °C) prepared from the PA-PLX-PA/HA aqueous solutions.

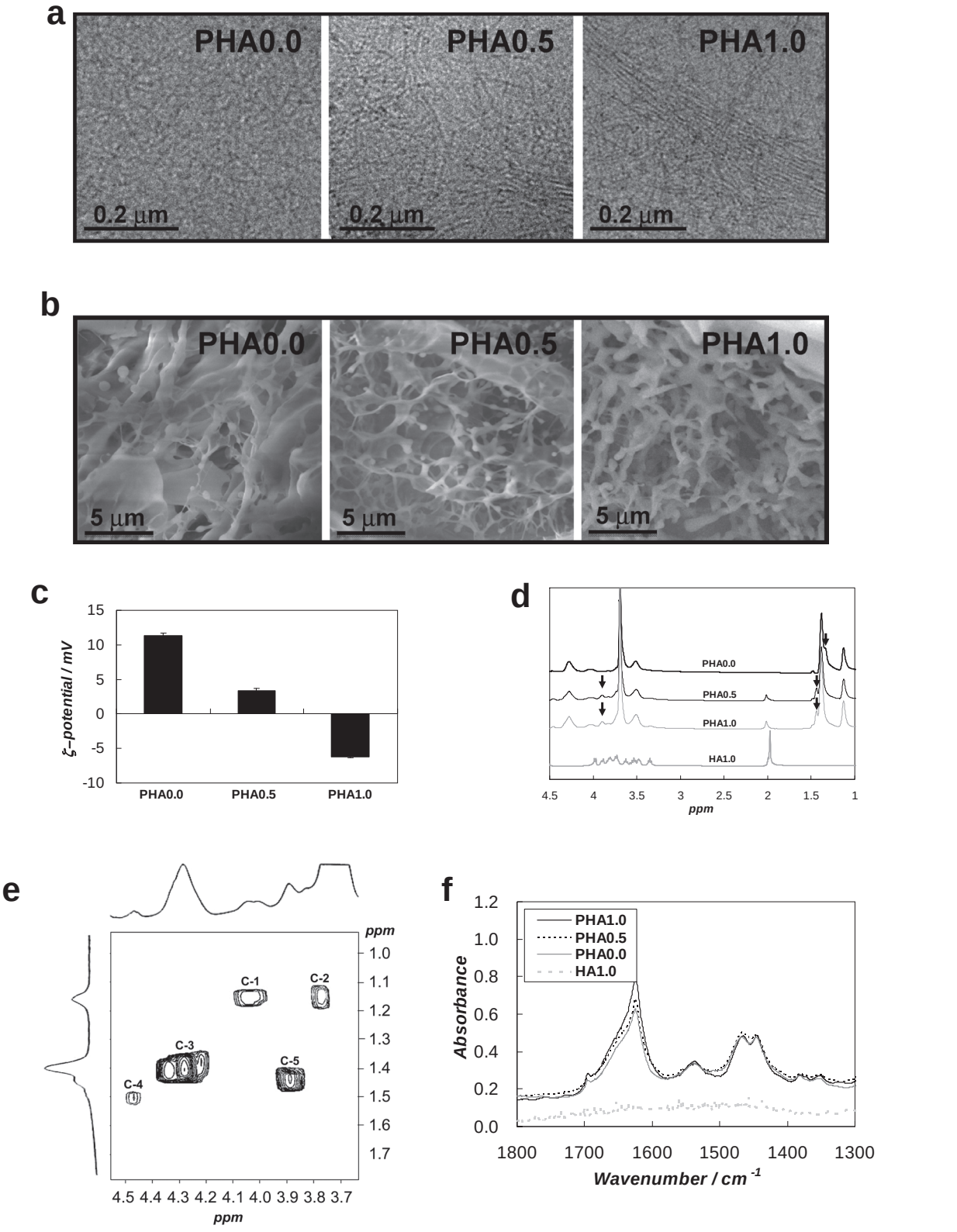

Figure 3. a) Cryo-TEM images and b) SEM images of PA-PLX-PA gels at 37 °C prepared from polymer aqueous solutions (8.0 wt%) as a function of HA content. PHAx indicates that *x* wt% of HA is incorporated in the PA-PLX-PA aqueous solution. c) Zeta-potential of PA-PLX-PA/HA aqueous solutions (1.0 wt%) as a function of HA content measured at pH = 7.4. d) ^{1}H-NMR spectra (D_2O) of PHA0.0, PHA0.5, PHA1.0, and HA at 37 °C. e) 2D-NMR (D_2O) spectra of PHA1.0 at 37 °C. f) FTIR (D_2O) spectra of PHA0.0, PHA0.5, PHA1.0, and HA at 37 °C. In the FTIR spectra of HA, the HA 1.0 wt% was used for comparison.

a specific orientation were observed in the gels containing 0.5 and 1.0 wt% HA (PHA0.5 and PHA1.0 in Figure 3a). The collagen nanofibers in the biological ECM showed a range of diameters from tens to hundreds of nanometers, and extend several micrometers in length.[21] Tendons consisting of collagen I are formed by thick fiber bundles, whereas the cartilage consisting of dominantly collagen II shows a loose and thin fibrils.[22] The alignment of the nanofibers also plays an important role in mechanical properties of the matrix against the stress direction, cell signalling, and proliferation of the cells. For example, when fibroblasts were cultured on the aligned nanofibers, the cells not only oriented in the fiber direction but also secreted more collagen, compared with the cells cultured on randomly aligned nanofibers.[23] Contact guidance theory suggests that cells tend to migrate in directions that are associated with structural properties of the substratum.[24] The efficiency of stress-bearing capacity (η) can be defined as $\eta = \Sigma a_n \cos^4\phi$, where a_n is the proportion of fibers lying along any given direction, and ϕ is the angle they form with the fiber axis.[25] When the fiber orientation and the stress direction are at a right angle, η would drop to its minimum.

In the current system, nanofibers with a thickness of 4–6 nm extend about one micrometer in a parallel way in the presence of HA, which is in contrast with the random orientation of the nanofibers in the absence of HA, indicating that the fiber orientation is induced by interactions between polyanionic HA and cationic rigid rod-flexible tail structured polypeptide block copolymers. The maximal linear dimension of a polypeptide with γ residues is 0.363γ nm,[26] that is 2.76 nm, therefore, the width of the fiber is about twice the linear dimension of PA. This calculation suggests that the PA of the PA-PLX-PA was not interdigitated and two PA blocks form the fiber in a parallel fashion, as presented in the Figure 1b.

The SEM images of the PA-PLX-PA/HA complex thermogels at 37 °C were obtained by quenching the thin films of the gels on the silicone wafer into liquid nitrogen (–190 °C), followed by freeze-drying the gels. SEM images of the gels show highly porous structures of both PA-PLX-PA and PA-PLX-PA/HA complex hydrogels (Figure 3b). The pores are occupied by water molecules in a hydrated gel state. The incorporation of hydrophilic HA into the PA-PLX-PA increases the swelling degree of the gel and, therefore, can induce more porous structure in a gel, which might decrease the gel modulus, as discussed previously.

To identify the nature of the interactions between PA-PLX-PA and HA, ζ-potential, NMR, and FTIR spectra of the complex were investigated. In the absence of HA, ζ-potential of PA-PLX-PA (PHA0.0) as an aqueous solution (1.0 wt%) was +11 mV, which in turn decreased to +3.4 mV (PHA0.5) and to –6.2 mV (PHA1.0) as the HA content increased (Figure 3c). The data support the ionic complex formation between the ammonium group of terminal alanine of PA-PLX-PA and the carboxylate (COO^-) groups of HA. ^{1}H-NMR spectra of the thermogels were investigated as a function of HA content at 37°C (Figure 3d). By adding HA to PA-PLX-PA, the methyl group of the terminal alanine of PA-PLX-PA, indicated by the arrows in Figure 3d, shifted from 1.33 ppm to 1.43 ppm, a new broad peak at 3.89 ppm appeared, and the HA peak at 1.97 ppm became broader and shifted to 2.00 ppm. To assign the spectral information and interpret the interactions between PA-PLX-PA and HA, homonuclear 2D-NMR spectra of PHA1.0 at 37 °C were acquired (Figure 3e).[27,28] The C-1 and C-2 came from the methyl/methine ($-CH_3$/-CH-) coupling and methyl/methylene ($-CH_3$/$-CH_2$-) coupling of the propylene glycol of PLX, respectively. C-3 was due to the methyl/methine ($-CH_3$/-CH-) coupling of the internal alanine of PA-PLX-PA. C-4 resulted from the methyl/methine ($-CH_3$/-CH-) coupling of the terminal alanine of PA-PLX-PA conjugated to solvent (OD^-) as shown by the peak at 4.47 ppm in the 1D ^{1}H-NMR spectra of PHA0.0 as well as PHA0.5, and PHA1.0. The new peak at 3.89 ppm (arrow in 1D ^{1}H-NMR) and the methyl group of the terminal alanine of PA-PLX-PA at 1.43 ppm (arrow in 1D ^{1}H-NMR) correlated to the C-5 in the 2D-NMR. Therefore, C-5 was assigned to the methyl/methine ($-CH_3$/-CH-) coupling resulting from the complex formation between the ammonium group of terminal alanine of PA-PLX-PA and the carboxylate (COO^-) groups of HA. Therefore, the new peak at 3.89 ppm in the 1D ^{1}H-NMR spectra was assigned to the methine (-CH-) group of the terminal alanine of PA-PLX-PA that interacted with the carboxylate group of HA. The following conclusions can be made based on these results: the change in chemical shift (1.33 to 1.43 ppm) and appearance of a new peak at 3.89 ppm in the ^{1}H-NMR spectra, and the C-5 with strong coupling in the 2D-NMR indicate that that the ammonium group on the terminal alanine of the PA-PLX-PA interacted with carboxylate of HA.

A strong band at 1626 cm^{-1} in the FTIR spectra[29] of the PA-PLX-PA/HA aqueous system indicated that the polypeptide (PA) predominantly forms β-sheet secondary structures in the complex thermogel (Figure 3f). The band intensity (absorbance) of the PA-PLX-PA/HA at 1626 cm^{-1} was substantially higher than that of PA-PLX-PA in the absence of HA, indicating that the β-sheet content of PA-PLX-PA increased by the complexation between HA and PA-PLX-PA.

To conclude, the PA-PLX-PA/HA ionic complex formation can be supported by the cryo-TEM images, zeta potential, NMR spectra, and FTIR spectra, as presented in the scheme (Figure 1b). Due to the rigid hydrophobic nature of PA and flexible hydrophilic nature of PLX, the PA-PLX-PAs form a core/shell structure. The ionic interactions between the ammonium ($-NH_3^+$) end groups of PA-PLX-PA and carboxylate ($-COO^-$) of HA lead to the formation of long fibers that tended to arrange in a parallel direction. Therefore, well-defined nanofibrous structures with a specific orientation are produced in the PA-PLX-PA/HA complex system.

As the temperature increased, the PA-PLX-PA aqueous solution turned into a gel. As reported previously, ^{13}C-NMR spectra (in D_2O) of the polymer showed collapsing and broadening of the PEG peak, and characteristic β-sheet band of the polymer at 218 nm in the circular dichroism spectra significantly strengthened as the temperature increased, suggesting that the sol-to-gel transition mechanism of the PA-PLX-PA aqueous solution is the dehydration of PEG and increases in β-sheet content of PA.[30] In PA-PLX-PA/HA complex system, the similar transition mechanism can be assumed except that the HA complexes with PA-PLX-PA.

The characteristics of chondrocytes cultured at 37 °C in the PA-PLX-PA/HA complex thermogels was investigated as a function of HA content. The cells suspended in the polymer aqueous solution were encapsulated in the gel by the temperature-sensitive sol-to-gel transition of the PA-PLX-PA/HA system. Matrigel (M in **Figure 4**) was also used as a reference scaffold. Proliferation of the chondrocytes significantly ($p < 0.01$) improved in

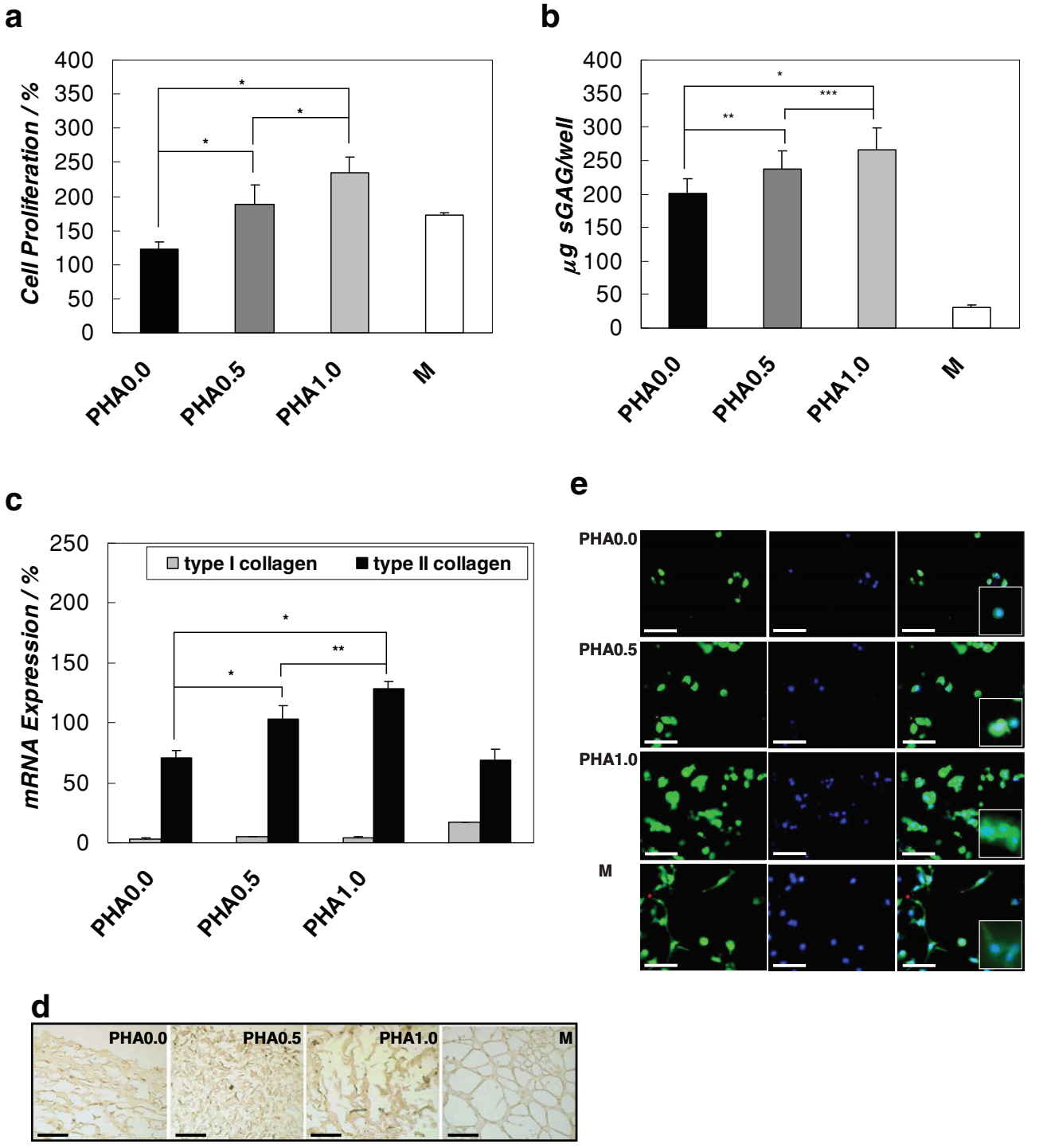

Figure 4. Effect of the HA content on the proliferation and biomarker expression of chondrocytes incubated for 14 days in hydrogels. Matrigel (M) is used for comparison. Asterisk (*) indicates $p < 0.01$ by the Student t-test. a) Proliferation of chondrocytes was analyzed by the CCK-8 method. 100% indicates the value at the day the 3D culture was started. b) Effect of the HA content on the amount of sGAG per well measured using the DMB assay. c) Effect of the HA content on the relative mRNA expression of type I and type II collagens. GAPDH was used as an internal control. d) Immunohistochemistry analysis of type II collagen (yellowish brown) produced by the chondrocytes encapsulated in the hydrogel. Dark brown spots are the nucleus of the cells. e) Fluorescence microscopy images of hydrogel encapsulating chondrocytes. The cytosols of cells (right) are stained using a Live (green)/Dead (red) kit, and the nuclei (blue) of cells (middle) are stained by Hoechst 33342. Overlapped images are shown in the right. Enlarged overlapped images are also inserted. The scale bar is 100 μm.

the presence of HA (PHA0.5 and PHA1.0) than in the absence of HA (PHA0.0) (Figure 4a). To investigate the differences in biomarker production in the PA-PLX-PA/HA thermogel as a function of HA content, sulfated glycosaminoglycan (sGAG) and mRNA expression of type I collagen and type II collagen were assayed. sGAG and type II collagen are typical biomarkers for articular cartilage formation.[31,32] Compared with chondrocytes cultured in PA-PLX-PA thermogels without HA (PHA0.0), the amount of sGAG was significantly ($p < 0.01$) increased in the presence of HA 1.0 wt% (PHA1.0) (Figure 4b). The mRNA expression of type II collagen was also significantly ($p < 0.01$) higher in the presence of 0.5 and 1.0 wt% HA than in the absence of HA (Figure 4c). In the immunostaining assay, the type II collagen (brown color) was prominent in the presence of HA, where the nuclei of the cells were also observed as dark brown spots (Figure 4d).

In 2D culture, mRNA expression of type I collagen was dominant relative to type II collagen.[18,33] In our 3D culture, mRNA expression of type II collagen was dominant over type I collagen, which again emphasizes the importance of 3D culture. The amount of sGAG and mRNA expression of type II collagen were significantly higher in the thermogelling PA-PLX-PA/HA complex system (PHA0.5 and PHA1.0) than the Matrigel™ system or the PA-PLX-PA system (PHA0.0). In the biological ECM, collagen nanofibers are dispersed in a proteoglycan-HA swollen hydrogel. HA is a major component of ECM in biological tissues including cartilage. HA is known to be involved in biological processes such as cell proliferation, wound repair, matrix organization, and morphogenesis.[34] Proliferation and spreading of the fibroblasts significantly increased in a 3D culture system of PEG diacrylate/HA interpenetrating network even in a low level (0.1–0.2%) of HA.[35] The cell-mediated enzymatic degradation of HA was claimed as the mechanism of the increased fibroblast activity. In addition, HA binds to receptors in cell membranes including CD44 and RHAMM, which activates intracellular signalling pathway to control the cell function.[36] In our current system, the addition of HA not only induced an orientation of the nanofibers through the ionic interactions with thermogelling polymers but also decreased the gel modulus due to the hydrophilic nature of HA. The modulus of the gel can affect the 3D culture of chondrocytes.[37,38] In the photo-crosslinked PEG dimethacrylate hydrogel, the production of GAG was most pronounced in the soft gel, whereas the expression of collagen type II and MMP were the highest in the hard gel.[38]

The improvement in cell proliferation and biomarker expression in the current PA-PLX-PA/HA matrix might come from a combination of the contributions through the above discussed biological functions, unique nanostructures, and modulus effects.

Live/Dead assay using fluorescence microscopy shows that the cells were healthy in the PHA0.0, PHA0.5, and PHA1.0 systems, where the live and dead cells appeared as green and red colors, respectively (Figure 4e). Live cells are distinguished by the presence of ubiquitous intracellular esterase activity, determined by the enzymatic conversion of the virtually nonfluorescent cell-permeant calcein AM to the intensely fluorescent calcein.[39,40] The polyanionic dye (calcein) is well retained within live cells, producing an intense uniform green fluorescence in live cells. Hoechst 33342 binds to the minor groove of double-stranded DNA of nucleus of the cell with a preference for sequences rich in adenine (A) and thymine (T), to give the image of the nucleus of the cell.[41] Although the dyes can bind to all nucleic acids, AT-rich DNA strands noticeably enhance fluorescence intensity. The overlapped images of the cytosol and nucleus supported that the fluorescence images came from the live cells (Figure 4e).

In addition, intercellular contacts and cell-clustering were also observed in the HA containing polypeptide thermogel. The preferential clustering in the PHA1.0 thermogel was noticeable. The organized matrix with a specific direction is known to provide biochemical cues for cell communication and signalling,[42,43] and consequently affect cellular processes.[44,45] In the Matrigel, chondrocytes lost their original spherical phenotype and adopted a fibrous morphology.

3. Conclusions

As a biocompatible and biodegradable polymer, HA has been investigated in drug delivery and tissue engineering applications.[46,47] To exploit HA as a biomimetic nanostructure-directing moiety, here we found that HA orientated a well-defined fibrous structure of amphiphilic block copolymers with a specific direction through the ionic interactions between the ammonium end group ($-NH_3^+$) of PA-PLX-PA and carboxylate groups ($-COO^-$) of HA. The in-situ formed biomimetic 3D culture system provided a compatible microenvironment for the encapsulated chondrocytes, where the cell clustering as well as improved cell proliferation and biomarker expression for articular cartilage were observed in the presence of HA relative to the absence of HA or in the Matrigel system.

This research emphasizes the importance of nanobiotechnology by providing a new method to develop a directional nanostructure through ionic interactions and proving its potential biomedical application.

4. Experimental Section

Dynamic Mechanical Analysis: The storage modulus of the polymer aqueous solutions (8.0 wt.) containing HA (0.0, 0.5, and 1.0 wt%) were investigated by dynamic rheometry (Rheometer RS 1; Thermo Haake) at 4 °C and 37 °C. The aqueous polymer solution was placed between parallel plates with 25 mm in diameter and a gap of 0.5 mm. During the dynamic mechanical analysis, the samples were placed inside a chamber with water-soaked cotton to minimize water evaporation. The data were collected under controlled stress (4.0 dyn/cm^2) and frequency of 1.0 rad/s.

Cryo-Transmission Electron Microscopy (Cryo-TEM): The cryo-TEM images of PA-PLX-PA aqueous solutions (8.0 wt%) containing 0.0, 0.5, and 1.0 wt% HA at 37 °C were obtained after equilibrating the solutions for 20 min at 37 °C. Vitrified specimens of polymer aqueous solutions were prepared on 200 mesh copper grids coated with a perforated form film (Ted Pella). A small drop (10 μL) was applied to the grid and blotted with filter paper to form a thin liquid film of solution, which was immediately plunged into liquid ethane at –170 °C. The procedure was performed automatically in the Vitrobot. The vitrified specimens were imaged on a FEI Tecnai G2 TEM, at 200 kV with a Gatan cryoholder maintained below –170 °C. Images were recorded on an Ultrascan 2K × 2K charge coupled device (CCD) camera. In the microscopes, images were recorded using the Digital Micrograph software package under low-dose conditions to minimize damage by the electron beam radiation.

Scanning Electron Microscopy (SEM): The SEM images of PA-PLX-PA aqueous solutions (8.0 wt%) containing 0.0, 0.5, and 1.0 wt% HA were obtained after the polymer solutions were dropped on the silicon wafer and kept at 37 °C in the oven for 20 min. Then, they were quenched into liquid nitrogen at –190 °C, and then freeze-dried. Scanning electron microscopy images were obtained by the field emission scanning electron microscopy (FE-SEM) instrument (JSM-6700F, JEOL Ltd., Japan).

3D Cell Culture: Chondrocytes were isolated from the knee articular cartilage of 4-week-old New Zealand white rabbits by collagenase digestion. Isolated chondrocytes were monolayer cultured in high glucose Dulbecco's modified eagle medium (DMEM) (Thermo Scientific, USA) containing 10% fetal bovine serum and 1% penicillin/streptomycin under a 5% CO_2 atmosphere at 37 °C and were subcultured in passage 2. Harvested cells (passage 3, 1.0×10^6 cells) mixed with PA-PLX-PA aqueous solutions (8.0 wt%; 0.25 mL) containing HA (0.0, 0.5, and 1.0 wt%), and Matrigel (as received) were incubated in 24-well culture plates at 37 °C for 30 min, during which chondrocytes were encapsulated by the sol-to-gel transition. DMEM (0.5 mL) containing 10% fetal bovine serum and 1% penicillin/streptomycin was added to the cell-encapsulated hydrogel under a 5% CO_2 atmosphere at 37 °C and the medium was replaced every three days. The proliferation of chondrocytes in hydrogels was assessed using the cell counting kit (CCK)-8 method. Each sample was analyzed in triplicate. The CCK-8 solution (0.8 mL; 10% v/v in medium, Dojindo, Japan) was added to each well. After 2 h of incubation, the absorbance value at 450 nm was measured using an ELISA reader (Model 550; Bio-Rad, Hercules, CA, USA), where absorbance at 655 nm was used for baseline correction. Hoechst 33342 (NucBlue Live Cell Stain: invitrogen, USA) was used to stain nucleus of the cell.

To determine the sGAG content in chondrocytes-encapsulated hydrogels, each sample was digested in papain solution. Then sGAG content was then measured using a 1,9-dimethyl-methylene blue (DMB) (Sigma-Aldrich, USA) assay in 96 well plates. Chondroitin sulfate C was used as a standard.

For immunohistochemistry of type II collagen, the cryo-sections were incubated with monoclonal antirabbit type II collagen antibody. Subsequently, antibody staining was detected using the Histostain-Plus kit (Invitrogen, USA) according to the manufacturer's protocol.

After 14 days of cell-culture, the total RNA content was extracted from the cell-encapsulated hydrogels using the TRI_{ZOL} reagent (Invitrogen, USA), according to the manufacturer's protocol. The extracted RNA pellet was dissolved in nuclease-free water, and the RNA quality and concentration were determined using the Experion system (Bio-Rad, CA, USA). After synthesizing the cDNA from the isolated RNA, real time polymerase chain reactions (PCR) were performed with the CFX96 system using the IQ SYBR Green Supermix. All samples were normalized based on the GAPDH level.

Viability of chondrocytes in hydrogels was determined using the Live/Dead kit. Chondrocytes encapsulating hydrogels were incubated at room temperature for 30 min in a solution of 4 mM ethidium homodimer-1 (EthD-1) and 2 mM calcein AM in phosphate buffered saline. Labelled cells were then viewed under a Nikon Eclipse E600 fluorescence microscope and images were captured using Lucia software. Viable cells were stained with calcein AM (green), while dead cells were stained with EthD-1 (red).

Supporting Information

Supporting information is available from the Wiley Online Library or from the author.

Acknowledgements

This research was supported by the National Research Foundation of Korea (NRF) grant funded by the MEST of Korea (Grant number: 2012-0000151, 2012-0000650, and R31-2008-000-10010-0).

Received: June 25, 2012
Published online: August 15, 2012

[1] Z. Huang, H. Lee, E. Lee, S. K. Kang, J. M. Nam, M. Lee, *Nat. Commun.* **2011**, *2*, 459.
[2] R. M. Capito, H. S. Azevedo, Y. S. Velichko, A. Mata, S. I. Stupp, *Science* **2008**, *319*, 1812.
[3] J. Luo, Y. W. Tong, *ACS Nano* **2011**, *5*, 7739.
[4] A. M. Kushner, Z. Guan, *Angew. Chem. Int. Ed.* **2011**, 50, 9026.
[5] M. K. Joo, M. H. Park, B. G. Choi, B. Jeong, *J. Mater. Chem.* **2009**, *19*, 5891.
[6] L. Yu, J. D. Ding, *Chem. Soc. Rev.* **2008**, *37*, 1473.
[7] X. J. Loh, J. Li, *Expert Opin. Ther. Pat.* **2007**, *17*, 965.
[8] C. Chun, H. J. Lim, K.-Y. Hong, K.-H. Park, S.-C. Song, *Biomaterials* **2009**, *30*, 6295.
[9] J. D. Kahmann, R. O'Brien, J. M. Werner, D. Heinegard, J. E. Ladbury, I. D. Campbell, A. J. Day, *Structure* **2000**, *8*, 763.
[10] V. C. Mow, R. Huiskes, *Basic Orthopaedic & Mechanobiology*, 3rd Ed., Lippincott Williams & Wilkins, Philadelphia, PA **2005**.
[11] T. Kameda, S. Takada, *Proc. Natl. Acad. Sci. USA* **2006**, *103*, 17765.
[12] J. Ngoenkam, A. Faikrua, S.Yasothornsrikul, J. Viyoch, *Inter. J. Pharm.* **2010**, *391*, 115.
[13] J. P. Chen, T. H. Cheng, *Macromol. Biosci.* **2006**, *6*, 1026.
[14] H. Sa-Lima, K. Tuzlakoglu, J. F. Mano, R. L. Reis, *J. Biomed. Mater. Res. Part A* **2011**, *98*, 596.
[15] K. Na, J. H. Park, S. W. Kim, B. K. Sun, D. G. Woo, H. M. Chung, K. H. Park, *Biomaterials* **2006**, *27*, 5951.
[16] H. Park, J. S. Temenoff, T. A. Holland, Y. Tabata, A. G. Mikos, *Biomaterials* **2005**, *26*, 7095.
[17] R. Censi, W. Schuurman, J. Malda, G. di Dato, P. E. Burgisser, W. J. A. Dhert, C. F. van Nostrum, P. di Martino, T. Vermonden, W. E. Hennink, *Adv. Funct. Mater.* **2011**, *21*, 1833.
[18] B. G. Choi, M. H. Park, S. H. Cho, M. K. Joo, H. J. Oh, E. H. Kim, K. Park, D. K. Han, B. Jeong, *Biomaterials* **2010**, *31*, 9266.
[19] Y. Jeong, M. K. Joo, K. H. Bahk, Y. Y. Choi, H. T. Kim, W. K. Kim, H. J. Lee, Y. S. Sohn, B. Jeong, *J. Controlled Release* **2009**, *137*, 25.
[20] B. G. Choi, M. H. Park, S. H. Cho, M. K. Joo, H. J. Oh, E. H. Kim, K. Park, D. K. Han, B. Jeong, *Soft Matter* **2011**, *7*, 456.
[21] G. Karp, *Cell and Molecular Biology*, 4th Ed., John Wiley & Sons, Inc., Hoboken, NJ **2005**.
[22] K. Kfihn, *Aesth. Plast. Surg.* **1985**, *9*, 141.
[23] Z. Ma, M. Kotaki, R. Inai, S. Ramakrishna, *Tissue Eng.* **2005**, *11*, 101.
[24] R. Bellairs, A. Curtis, G. Dunn, *Cell Behavior*, Cambridge University Press, Cambridge, UK **1982**.
[25] V. Ottani, M. Raspanti, A. Ruggeri, *Micron* **2001**, *32*, 251.
[26] T.E. Creighton, *Proteins-Structures and Molecular Properties*, 2nd Ed., W. H. Freeman and Company, New York **1993**.
[27] I. Fernandez, E. Martinez-Viviente, P. S. Pregosin, *Inorg. Chem.* **2005**, *44*, 5509.
[28] P. S. Pregosin, *Pure Appl. Chem.* **2009**, *81*, 615.
[29] E. H. Kim, M. K. Joo, K. H. Bahk, M. H. Park, B. Chi, Y. M. Lee, B. Jeong, *Biomacromolecules* **2009**, *10*, 2476.
[30] H. J. Oh, M. K. Joo, Y. S. Sohn, B. Jeong, *Macromolecules* **2008**, *41*, 8204.
[31] C. Vinatier, D. Magne, P. Weiss, C. Trojani, N. Rochet, G. F. Carle, C. Vignes-Colombeix, C. Chadjichristos, P. Galera, G. Daculsi, J. Guicheux, *Biomaterials* **2005**, *26*, 6643.
[32] J. Kisiday, M. Jin, B. Kurz, H. Hung, C. Semino, S. Zhang, A. J. Grodzinsky, *Proc. Natl. Acad. Sci. USA* **2002**, *99*, 9996.
[33] J. M. Kemppainen, S. J. Hollister, *Biomaterials* **2010**, *31*, 279.
[34] J. A. Burdick, G. D. Prestwich, *Adv. Mater.* **2011**, *23*, H41.
[35] J. K. Kutty, E. Cho, J. S. Lee, N. R. Vyavahare, K. Webb, *Biomaterials* **2007**, *28*, 4928.
[36] X. Xu, A. K. Jha, D. A. Harrington, M. C. Farach-Carson, X. Jia, *Soft Matter* **2012**, *8*, 3280.
[37] J. A. Burdick, C. Chung, X. Jia, M. A. Randolph, R. Langer, *Biomacromolecules* **2005**, *6*, 386.

[38] G. D. Nicodemus, S. C. Skaalure, S. J. Bryant, *Acta Biomater.* **2011**, *7*, 492.
[39] F. Ito, K. Usui, D. Kawahara, A. Suenaga, T. Maki, S. Kidoaki, H. Suzuki, M. Taiji, M. Itoh, Y. Hayashizaki, T. Matsuda, *Biomaterials* **2010**, *31*, 58.
[40] H. Park, J. S. Temenoff, Y. Tabata, A. I. Caplan, R. M. Raphael, J. A. Jansen, A. G. Mikos, *J. Biomed. Mater. Res.* **2009**, *88A*, 889.
[41] L. Wu, J. C. H. Leijten, N. Georgi, J. N. Post, C. A. van Blitterswijk, M. Karperien, *Tissue Eng. Part A* **2011**, *17*, 1425.
[42] D. A. Albrecht, G. H. Underhill, T. B. Wassermann, R. L. Sah, S. N. Bhatia, *Nat. Methods* **2006**, *3*, 369.
[43] P. Szafranski, S. A. Goode, *Development* **2004**, *131*, 2023.
[44] E. S. Place, N. D. Evans, M. M. Stevens, *Nat. Mater.* **2009**, *8*, 457.
[45] W. J. Chung, J. W. Oh, K. Kwak, B. Y. Lee, J. Meyer, E. Wang, A. Hexemer, S. W. Lee, *Nature* **2011**, *478*, 364.
[46] J. A. Burdick, G. D. Prestwich, *Adv. Mater.* **2011**, *23*, H41.
[47] E. J. Oh, T. Park, K. S. Kim, J. A. Yang, J. H. Kong, M. Y. Lee, A. S. Hoffman, S. K. Hahn, *J. Controlled Release* **2010**, *141*, 2.